NeuroImage 195 (2019) 232–242

Contents lists available at ScienceDirect

NeuroImage

journal homepage: www.elsevier.com/locate/neuroimage

# Distinct visuo-motor brain dynamics for real-world objects versus planar images

Francesco Marini [a,b,*], Katherine A. Breeding [a], Jacqueline C. Snow [a,**]

[a] Department of Psychology, University of Nevada, 1664 N Virginia St, Reno, NV, 89557-0296, USA
[b] Swartz Center for Computational Neuroscience, University of California San Diego, 9500 Gilman Drive, La Jolla, CA, 92093-0559, USA

ARTICLE INFO

*Keywords:*
Real-world objects
Images
EEG
Mu rhythm

ABSTRACT

Ultimately, we aim to generalize and translate scientific knowledge to the real world, yet current understanding of human visual perception is based predominantly on studies of two-dimensional (2-D) images. Recent cognitive-behavioral evidence shows that real objects are processed differently to images, although the neural processes that underlie these differences are unknown. Because real objects (unlike images) afford actions, they may trigger stronger or more prolonged activation in neural populations for visuo-motor action planning. Here, we recorded electroencephalography (EEG) when human observers viewed real-world three-dimensional (3-D) objects or closely matched 2-D images of the same items. Although responses to real objects and images were similar overall, there were critical differences. Compared to images, viewing real objects triggered stronger and more sustained event-related desynchronization (ERD) in the μ frequency band (8–13 Hz) – a neural signature of automatic motor preparation. Event-related potentials (ERPs) revealed a transient, early occipital negativity for real objects (versus images), likely reflecting 3-D stereoscopic differences, and a late sustained parietal amplitude modulation consistent with an 'old-new' memory advantage for real objects over images. Together, these findings demonstrate that real-world objects trigger stronger and more sustained action-related brain responses than images do. The results highlight important similarities and differences between brain responses to images and richer, more ecologically relevant, real-world objects.

## 1. Introduction

Current knowledge of the cognitive and neural basis of human visual perception has been established predominantly by studies that have used stimuli in the form of planar images. Although this approach has yielded important insights into image vision, the human brain presumably has evolved to allow us to perceive and interact with real objects in naturalistic environments (Gibson, 1979). Despite the fundamental differences between real objects and images, the overarching assumption in cognitive neuroscience research has been that images are equivalent to their real-world counterparts. This basic assumption is rarely recognized or acknowledged. For example, many report studying real-world or graspable objects (Brady et al., 2008, 2016; Handy et al., 2003; Konkle et al., 2010; Konkle and Oliva, 2011, 2012; Lee et al., 2012; McNair et al., 2017; Nako et al., 2015; Khaligh-Razavi et al., 2018), yet representations of objects are neither real, nor do they offer genuine affordances.

Emerging evidence from cognitive psychology has begun to challenge the assumption of equivalence between real objects and images. Compared to 2-D images of objects, real-world objects elicit different gaze patterns in infants (Gerhard et al., 2016), facilitate object recognition (Chainay and Humphreys, 2001; Humphrey et al., 1994), enhance memory (Snow et al., 2014), increase attentional capture (Gomez et al., 2017), and bias valuation and decision-making (Romero et al., 2018). These unique effects of real objects on behavior are thought to be driven at the neural level by format-specific increases in the strength and/or duration of activation in visuo-motor networks involved in automatic planning of motor actions (Cisek and Kalaska, 2010; Gallivan et al., 2009; Gomez et al., 2017). However, no studies to date have tested this hypothesis. Although evidence from fMRI suggests that the format in which a stimulus is displayed influences neural responses across successive object presentations (Snow et al., 2011), this leaves open the critical question of whether, and how, real objects modulate cortical brain dynamics at the level of individual occurrences, independently of previous presentations (Cisek and Kalaska, 2010; Gallivan et al., 2009, 2011a;

* Corresponding author. University of Nevada, Department of Psychology, 9500 Gilman Drive, La Jolla, CA 92093-0559, United States.
** Corresponding author. Department of Psychology, University of Nevada, 1664 N Virginia St, Reno, NV, 89557-0296, USA.
*E-mail addresses:* francesco.pd@gmail.com (F. Marini), snow@unr.edu (J.C. Snow).

https://doi.org/10.1016/j.neuroimage.2019.02.026
Received 29 August 2018; Received in revised form 26 January 2019; Accepted 9 February 2019
Available online 15 February 2019

Gomez et al., 2017).

Unlike fMRI, in which blood oxygenation level dependent (BOLD) contrast detects vascular responses that lag the underlying neural events by seconds (Logothetis et al., 2001), electroencephalography (EEG) measures electrical changes at the surface of the scalp with millisecond-precision and can therefore provide fine-grained information about the time-course of cortical dynamics (e.g., Makeig et al., 2002). The EEG signal can be decomposed to reveal frequency-specific changes associated with cognitive processes (Basar et al., 1999; Klimesch, 1999). One such process is the transformation of visual object information into action representations, which is reflected by desynchronization of the μ ('mu') rhythm (8–13Hz) (Pineda, 2005). Desynchronization (including α, μ and β rhythms) is a reliable correlate of activated cortical networks (Pfurtscheller, 2001) and is directly related to fMRI BOLD response amplitude (Laufs et al., 2003). The rolandic μ rhythm originates in primary sensorimotor and premotor cortex and is recorded over central electrodes (Pfurtscheller et al., 1997). Typically, μ desynchronization occurs during both preparation and execution of self-initiated hand actions, as well as when hand actions are visually observed or imagined (Hari, 2006; Muthukumaraswamy and Johnson, 2004; Muthukumaraswamy et al., 2004; Pfurtscheller et al., 1997; Pineda, 2005). Observation of images of manipulable objects, such as tools, also elicits desynchronization of the μ rhythm over sensorimotor networks (Proverbio, 2012; Suzuki et al., 2014).

Here, we used EEG to contrast how cortical brain dynamics unfold when right-handed human observers view everyday real-world graspable objects versus 2-D images of the same items. Previous studies have shown that viewing images of graspable objects can automatically trigger motor preparation responses (Proverbio et al., 2011; Proverbio, 2012; Wamain et al., 2016). Given that real objects afford genuine motor actions, whereas images do not, we predicted that real objects would trigger stronger and more prolonged motor preparation signatures compared to 2-D images of the same items. We also predicted that the motor preparation signals for real objects would be stronger in the left hemisphere, contralateral to the dominant (right) hand. To pre-empt the results, we found that although there were similarities in overall neural responses to both stimulus formats, real objects elicited perceptual and neural responses that were distinct from those elicited by 2-D images. Specifically, real objects elicited a stronger and longer desynchronization in the μ frequency band, particularly over the left hemisphere. Real objects (versus 2-D images) also elicited differences in early and late event-related potential (ERP) amplitudes over occipital and parietal electrodes, corresponding to known signatures of stereoscopic disparity (Pegna et al., 2017) and memory (Donaldson and Rugg, 1999; Friedman and Johnson, 2000; Harris and Wilcox, 2009; Rugg and Curran, 2007; Rugg et al., 1998; Schendan and Kutas, 2003; Voss and Paller, 2008), respectively. Importantly, we show that the early difference in ERP amplitudes over occipital areas are dissociable from subsequent amplitude and frequency effects recorded over dorsal cortex. Together, our results confirm that real-world objects trigger neural signatures that are distinct from those of planar images.

## 2. Material and methods

### 2.1. Experimental procedure

#### 2.1.1. Participants

Twenty-four right handed healthy University of Nevada Reno students (mean age ± SD: 25.7 ± 7.5, 10 males) volunteered for the experiment. All participants reported normal or corrected-to-normal vision, no history of neurological impairments, and gave both written and oral informed consent as required by the university Institutional Review Board.

#### 2.1.2. Setup and stimuli

Stimuli consisted of 96 real-world objects and 96 2-D photographs of the same items, including 16 kitchen tools (i.e., knife) and 16 garage tools (i.e., flashlight), with 3 exemplars each (i.e., 3 different knives, 3 flashlights, etc.) (Fig. 1A and Supplementary Fig. 1). Each real-world object was mounted at the center of a 10 × 14 in. matte black foam-core board with the handle facing rightward. High-resolution photographs were taken of each mounted object, then printed in high-resolution and attached on 10 × 14 in. matte black foam-core boards (Fig. 1A). Magnets were glued to the back of foam-core boards and in corresponding positions on the faces of a custom-built rotating drum (22× 14 in.), which was used for stimulus display.

#### 2.1.3. Behavioral paradigm

Participants were seated 16 in. from the rotating drum with their eyes aligned to the center and wore earphones throughout the experiment to mask any extraneous noise. Stimulus presentation was controlled using computer-controlled PLATO visual occlusion spectacles (Translucent Technologies Inc.) that switched between 'closed' (opaque) and 'open' (transparent) states with ±3 ms accuracy assessed with a timing test (n = 1000, 95% CI). Each trial started with a 300 ms high-pitch tone (880 Hz). After a variable delay (800–1600 ms, selected randomly from a uniform distribution) the spectacles opened, revealing the stimulus for 800 ms. After another variable delay (1200–1800 ms), a 150 ms low-pitch tone (440 Hz) prompted participants to make a verbal response. In order to sustain participant engagement, we asked observers to rate: 'how much physical effort would it take to use this specific object according to its normal function?', on a scale from 1 (not effortful; e.g., a teaspoon) to 10 (very effortful; e.g. a hand drill) (Fig. 1B). Importantly, to prevent known action-related differences (Freud et al., 2017) from contaminating our results, our task involved neither an object interaction nor a manual response. There were 192 trials in the experiment (96 real-world objects and 96 images, each presented once). The stimuli were presented in a randomized sequence in 8 separate blocks of 24 trials each, with short breaks in-between blocks.

Three experimenters conducted each testing session: one controlled stimulus presentation and timing; the second helped select stimuli for upcoming trials and manually entered participants' responses; the third managed and monitored the electrophysiological recordings (see below). The experimenters worked behind black curtains that surrounded the display apparatus; only the front face of the drum was visible to participants during the study. Written and verbal instructions were provided, and 4 practice trials were conducted, prior to the main experiment. Timing of stimulus presentation, and the real-time encoding of events in the electrophysiological recordings (see below), were controlled using Matlab R2016a (Mathworks, Inc.) and Psychtoolbox 3.0.13 (Kleiner et al., 2007). The entire session, including mounting of electrodes, lasted ~2.5 h.

### 2.2. Data analysis

The complete dataset, as well as the Matlab scripts that were used to analyze the data and generate the figures included in this paper, have been made available through a separate publication (Marini et al., 2019).

#### 2.2.1. Behavioral analysis

Behavioral data of effort-to-use were transformed in Z-scores (within subject). Behavioral effort ratings were sorted based on individual items. Two values were obtained for each item, one value was collected when the item was presented as real object and the other when presented as image. A Pearson correlation analysis was conducted (Fig. 1C, left). For the right graph in Fig. 1C, effort ratings were sorted based on individual subjects and display format (Real, Image), and analyzed using a paired *t*-test (two-tailed).

#### 2.2.2. EEG recording and preprocessing

EEG was recorded with a 128-channel Biosemi ActiveTwo system using 128 head electrodes plus four electrooculogram electrodes and two (i.e., left and right) mastoid electrodes. Analyses were conducted in

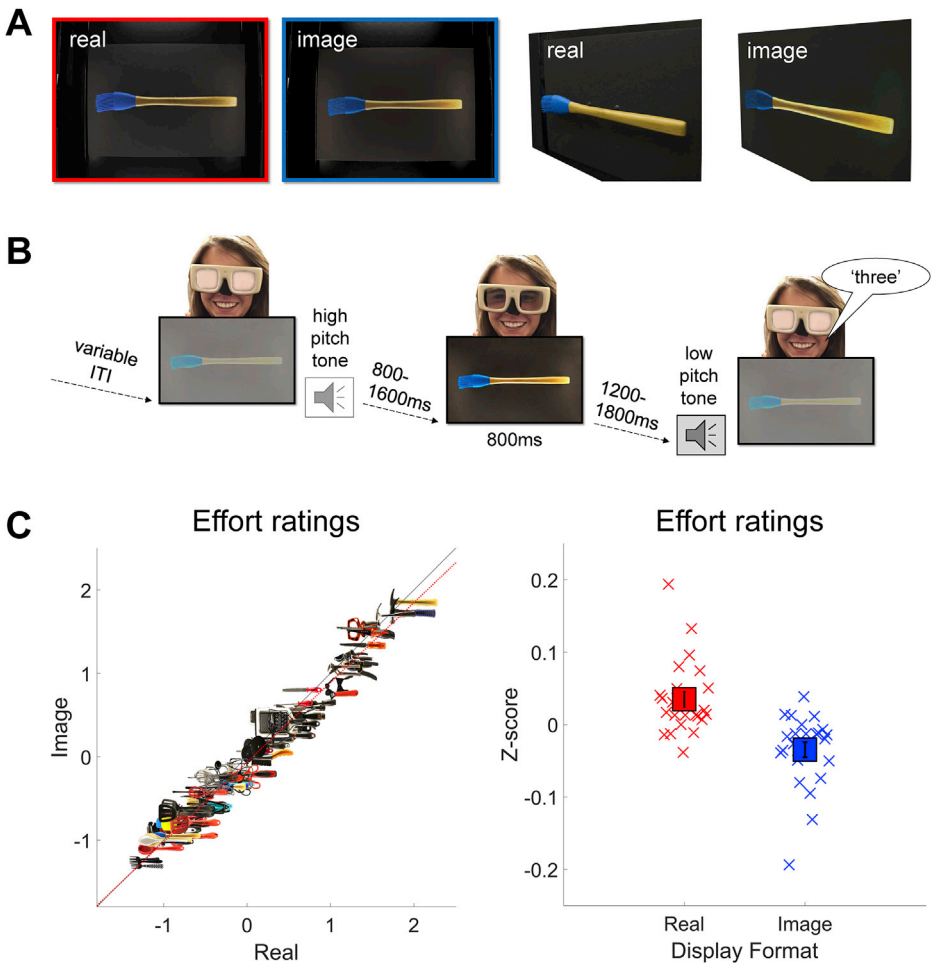


**Fig. 1. Experimental setup and behavioral results.**

*Panel A.* Example of a stimulus object (basting brush) as shown in the real object (left) and 2-D image (right) conditions, viewed from the observer's canonical perspective. The same stimuli are also shown from an oblique perspective (rightmost panels); when viewed from front-on, the real object and image stimuli were closely matched for apparent size, distance, background, illumination and color.

*Panel B.* Trial sequence. PLATO liquid-crystal occlusion spectacles were used to control stimulus presentation and timing throughout all trials with millisecond accuracy. After a variable-duration inter-trial interval (ITI), an auditory high-pitch tone signaled trial onset. After a delay (800–1600 ms) the PLATO glasses opened (transparent state) for 800 ms. The PLATO glasses then closed (opaque state), and after a second delay (1200–1800 ms), a low-pitch tone signaled to the participant to make his/her response. The participant's task was to rate verbally (on a scale from 1 to 10) how effortful it would be to use the object according to its typical function.

*Panel C.* Left: Analysis of subjective effort ratings for each object (averaged across participants). Although the item ratings were highly correlated across display formats, higher-effort items were perceived as being more effortful to use when they were presented as real objects versus images (the dotted red line represents the least-square best fit and the dotted black line is the unity slope line). Right: Analysis of effort ratings by participants (averaged across object identity). Real objects were perceived as being more effortful-to-use compared to when they were viewed as images.

Matlab using EEGLAB 14.1.1 (Delorme and Makeig, 2004). Signals were re-referenced to the mastoids average and bandpass filtered (1–100 Hz). Noisy channels were interpolated, line noise was attenuated, and epochs were created from −800 ms to 2000 ms relative to stimulus onset. Epochs containing artifacts were rejected using a voltage-based threshold. Independent-component analysis (ICA) was performed (Makeig et al., 1996). ICs containing artifacts (i.e., eye movements, muscular activity, etc.) were identified manually and rejected.

### 2.2.3. ERSP power analysis

The power of the event-related spectral perturbation (ERSP) was computed using Morlet wavelets as implemented in newtimef function in EEGLAB. To compare the sensorimotor μ rhythm in response to visually-presented real objects and images (Figs. 2 and 5B), we averaged baseline-corrected (time interval from −500 ms to 0 ms) ERSP power from a cluster of central electrodes (Biosemi electrodes A1, A2, A3, B1, B2, C15, C16). This central electrode cluster has been widely used to measure the sensorimotor μ rhythm in object perception tasks (Behmer and Jantzen, 2011; Nystrom et al., 2011; Perry and Bentin, 2009; Perry et al., 2011; Pfurtscheller et al., 2006; Pineda et al., 2011; Proverbio, 2012; Wamain et al., 2016, 2018). For the analysis of lateralized μ rhythm, we used one left-hemisphere and one right-hemisphere electrode located in the C3 and C4 positions of the International 10–20 System, which correspond to hand areas in the human primary motor cortex (Homan et al., 1987; Pfurtscheller et al., 1997; Neuper and Pfurtscheller, 2001). For all ERSP analysis a divisive baseline was used, in line with a gain model (Grandchamp and Delorme, 2011). Single-trial ERSP power was averaged across electrodes first, then across objects and, for illustration purposes, the 10*log10 transformation was applied to the average of ERSP power across trials prior to the subtraction between real and image conditions (the subtraction in log-space corresponds to the division between non-log power values and therefore this method is in keeping with our gain model approach). Statistical comparisons across display formats in the central electrode cluster were conducted using a cluster-based permutation test (n=10000; intensity threshold for cluster formation $\alpha = 0.001$, cluster size threshold $\alpha = 0.05$). Moreover, a-priori statistical comparisons across display formats were conducted, separately for the C3 and C4 electrode data, using a cluster-based permutation test (same parameters as above).

### 2.2.4. Correlation analysis

A brain-behavior correlation analysis was conducted to investigate whether changes in μ or β-band event-related desynchronization (ERD) were explained by differences in perceived effort-to-use. The average ERSP power within 1-Hz frequency bins at central electrodes (same electrodes as ERSP power analysis) was correlated across items with the behavioral effort ratings. The frequency range used for this analysis was 8–25Hz and the time range was 0–1600 ms (80 ms-wide sliding window, step-size 40 ms). This yielded 720 Pearson correlations for each condition (real, image), of which only 360 were independent because of time window overlap. To address the problem of multiple comparisons, using a Bonferroni-corrected significance threshold would have yielded a corrected-$\alpha = 0.0001$. Instead, we used a more lenient (uncorrected) threshold $\alpha = 0.001$ in order to increase detection power and maximize the likelihood of identifying possible relationships between the behavioral and neural data.

### 2.2.5. Mass univariate analysis of event-related potentials (ERP)

Data for ERP analyses (Fig. 3, **4**, **5A**, and **5C**) were segmented in

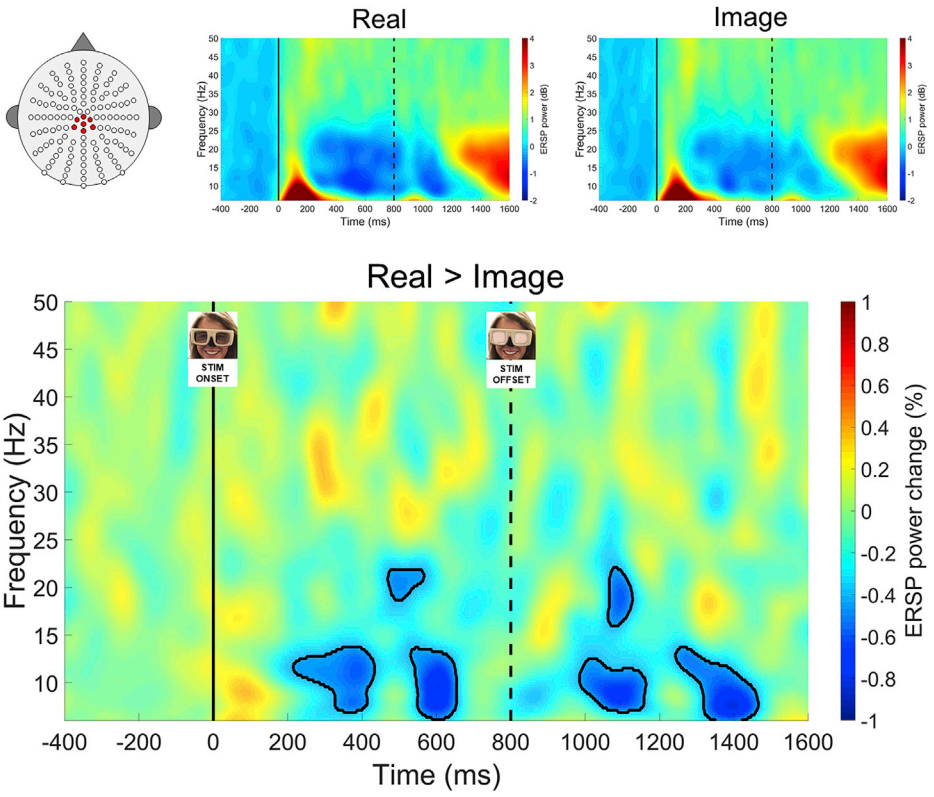


**Fig. 2. Comparison of time-frequency power across display formats.**
Time-frequency power of the event-related spectral perturbation (ERSP) over central electrodes (shown on topographic map, top left) averaged across all participants and objects. Upper panels show log-power spectra separately for real objects (left) and images (right), averaged across all trials. Lower panel illustrates the difference between the upper panels, corresponding to the difference between conditions (real minus image) in the average log-power. Event-related desynchronization was significantly stronger for real objects relative to images within several time-frequency regions (identified via cluster-based permutation analysis; black outlines in the lower spectral graph represent areas of statistical significance, see Supplementary Table 1). Vertical solid and dashed lines denote time of stimulus onset and offset, respectively.

shorter epochs (from −200 ms to 800 ms relative to stimulus onset) and baseline-corrected (from −200 ms to 0 ms). The analysis used the mass-univariate toolbox in Matlab (Blair and Karniski, 1993; Groppe et al., 2011; Guthrie and Buchwald, 1991). Statistical significance was evaluated in the time-range 50–800 ms post-stimulus using the cluster mass permutation test (cluster formation threshold $\alpha = 0.01$, significance threshold $\alpha = 0.05$). In order to determine what electrode channels were considered spatial neighbors, and therefore attributed to the same cluster, we used the default settings of the mass univariate toolbox ('chan_hood' = 0.61; Groppe et al., 2011). The mass univariate ERP analysis identified two regions of adjacent significant electrodes and/or time-points (Supplementary Table 3) that were used for the subsequent analysis.

#### 2.2.6. Late parietal ERPs analysis

The analysis of late parietal ERPs based on presentation order and display format (Figs. 4 and 5C) used the average ERP amplitude (computed separately for each display format and presentation order) from significant time-points and electrodes in the late parietal cluster from the mass univariate analysis. Because each object was presented twice across the whole experiment (once as real object and once as an image), one out of two possible pairs of presentation orders occurred for each item (the first time as an image and the second as a real object, or vice-versa). The 'old-new' ERP effect was computed as the difference wave for each item (second minus first presentation). A 2 × 2 repeated-measure analysis of variance factoring Presentation Order and Display Format was conducted on mean amplitudes extracted from the time points and electrodes of the late parietal cluster.

## 3. Results

### 3.1. Objects are rated as more effortful-to-use when viewed as real exemplars versus images

Effort ratings for each object were correlated across display formats. As apparent from Fig. 1C (left), individual item ratings were evenly distributed from low- (i.e., fork, spoon, spatula) to high-effort (i.e., hammer, handsaw, clamp) objects. Moreover, there was a strong correlation between effort ratings for real objects and images ($r = 0.985$, $p < .001$; Fig. 1C, left), reflecting comparable task requirements between display formats. Surprisingly, however, the correlation coefficient was significantly lower than 1 [$t(94) = 2.971$, $p = .002$], indicating that higher-effort real objects were rated as being more effortful to use than the corresponding images. Similarly, a contrast of effort ratings at the level of participants revealed that real-objects were perceived as being more effortful to use than their images [$t(23) = 3.349$, $p = .003$; Fig. 1C, right], even though no manual actions were explicitly planned or initiated towards any of the stimuli. Critically, however, as we show below, these differences in behavioral ratings for real objects and images were *not* correlated with differences in the brain dynamics across stimulus formats (Fig. 3), suggesting that the cortical modulations were not attributable to the task requirements.

### 3.2. Stronger and more prolonged μ desynchronization for real-world objects versus images

To determine whether real objects increase the strength or duration of activation in brain networks involved in automatic action planning, we first compared the magnitude and time-course of μ rhythm desynchronization across display formats. To do this, we contrasted format-dependent changes in event-related spectral perturbation (ERSP: Makeig, 1993) power within central electrodes over parietal cortex (Wamain et al., 2016). We searched for differences in ERSP from stimulus onset up to 800 ms post stimulus-offset (Fig. 2). We expected to observe event-related desynchronization (ERD) in the μ band that is greater in magnitude, and that extends longer over time, for real objects versus images. In line with this prediction, stronger μ ERD for real objects (versus images) was observed in several time-frequency clusters, ranging from ~220 ms to 1400 ms post stimulus onset (cluster-based permutation test: $n = 10000$, intensity threshold for cluster formation $\alpha = 0.001$, cluster size threshold $\alpha = 0.05$; Fig. 2 and Supplementary Table 1).

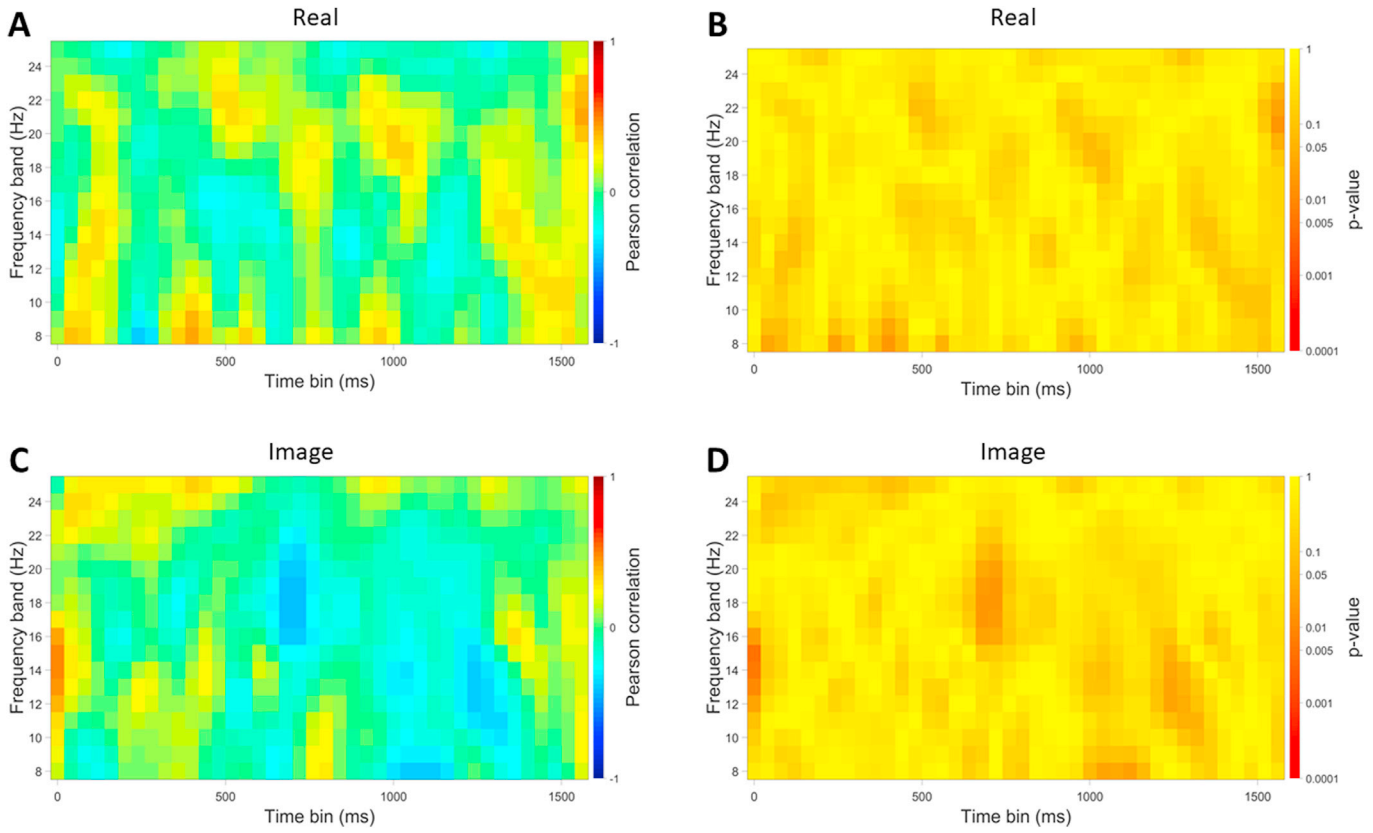


**Fig. 3. Brain-behavior correlations.** Time-frequency representation of Pearson correlation coefficients (panels **A** and **C**) and corresponding p-values (panels **B** and **D**, respectively) for an item-based correlation analysis between ERSP power (averaged across the central electrode cluster used for the ERSP analysis) and behavioral effort ratings (panels **A**, **B**: real objects, panels **C**, **D**: images). We used an uncorrected threshold rather than a conventional correction for multiple comparison in order to adopt a more lenient criterion and increase detection power (significance threshold > .001, uncorrected for multiple comparisons). No regions of the time-frequency space showed a significant correlation between ERSP power and effort ratings.

Greater ERD for real-objects versus images was also found in the β frequency band, which is known to show greater ERD during movement planning and execution (Turella et al., 2016; Zaepffel et al., 2013). Importantly, the reverse effect - i.e., larger event-related *synchronization* (ERS) – for real objects versus images was not observed at any time point or frequency within the analyzed time-window, thus attesting to the directional specificity of the observed time-frequency perturbations. Control analyses (Fig. 3) revealed no item-based correlations between the magnitude of ERD and behavioral effort ratings, indicating that the stronger ERD for real objects (versus images) could not be explained by differences in perceived effort-to-use across the two display formats.

Next, we examined whether there was a lateralized bias in the strength of motor preparation signals for real objects versus images in our right-handed observers. We predicted that if the increased μ desynchronization for real objects (versus images) reflects stronger motor preparation to act, then this pattern should be most apparent over motor cortex in the left hemisphere, contralateral to the dominant hand. Conversely, there should be little, if any, difference in the strength of μ desynchronization across the two display formats over motor cortex in the right hemisphere. To test this prediction we contrasted ERD for real objects versus images, separately at electrodes located over the left and right-hemisphere hand area (Pfurtscheller et al., 1997; Neuper and Pfurtscheller, 2001). Over the left-hemisphere hand area ERD was significantly stronger for real objects (versus images) in several time-frequency clusters (cluster-based permutation test: $n = 10000$, intensity threshold for cluster formation $\alpha = 0.001$, cluster size threshold $\alpha = 0.05$; see Fig. 4A and Supplementary Table 2); conversely, there was no significant difference in ERD for real objects versus images over right motor cortex (see Fig. 4B).

### 3.3. Real objects and images elicit different early and late ERPs

Next we examined whether real objects and images elicit differences in ERPs. ERPs reveal information about the average time-course of waveforms whose phase is reset at the onset of each stimulus. Rather than restricting the ERP analysis to a-priori temporal windows or scalp locations, we used a mass univariate analysis to contrast ERPs to real objects versus images together with cluster-based permutation statistics (Groppe et al., 2011). The strength of this approach is that it compares responses across time-points and electrodes without imposing temporal or spatial constraints on the investigated effects, while correcting for multiple comparisons (Maris and Oostenveld, 2007).

Importantly, images of objects presented with stereoscopic disparity have been shown to elicit greater negativity of early ERPs than those presented non-stereoscopically (Pegna et al., 2017). Given that real objects, when viewed binocularly, convey stereo depth information whereas 2-D images do not (e.g., Harris and Wilcox, 2009), we expected to observe similar disparity-related ERP effects. Accordingly, more negative ERPs for real objects versus 2-D images were observed over occipital electrodes starting at ~100 ms after stimulus onset (cluster-based permutation test, $n = 1000$, $p < .05$; Fig. 5 and Supplementary Table 3).

In addition, however, larger amplitudes for images (versus real objects) were *also* observed in late ERPs over parietal cortex at latencies between ~550 ms and 800 ms (cluster-based permutation test, $n = 1000$, $p < .05$; Fig. 5 and Supplementary Table 3). The spatio-temporal nature of this ERP corresponds with the late extended positivity frequently observed for objects that have been viewed previously (i.e., 'old') relative to newly presented items (the 'old/new effect') (Rugg and Curran, 2007). To examine this result further, we investigated whether the late parietal

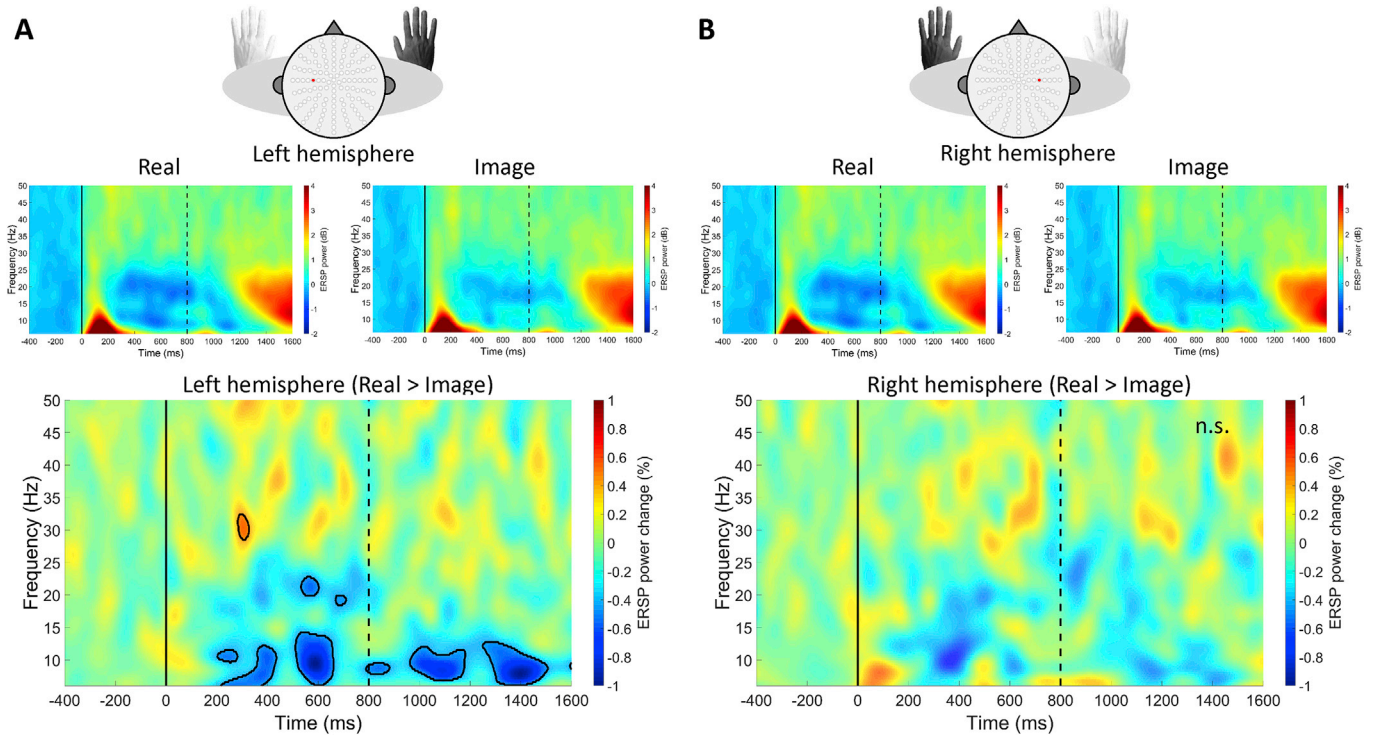


**Fig. 4. Lateralized bias in the strength of motor preparation signals.** Time-frequency power of the event-related spectral perturbation (ERSP) for electrodes (shown on topographic maps) over the putative left (panel A) and right motor cortex (panel B) averaged across all participants and objects. Upper panels show log-power spectra separately for real objects and images, while lower panel illustrates the difference between the upper panels, corresponding to the difference between conditions (real minus image) in the average log-power for the left and right hemisphere (panels **A** and **B**, respectively). Event-related desynchronization was significantly stronger for real objects relative to images in the left hemisphere (identified via cluster-based permutation analysis; black outlines in the lower spectral graph represent areas of statistical significance, see Supplementary Table 2; n.s.: not significant). Vertical solid and dashed lines denote time of stimulus onset and offset, respectively.

ERP difference between real objects and images was related to the order in which the stimuli in each display format were viewed. Each object in our study was presented twice, once as a real object and once as an image (see *Methods*). As such, we conducted a fine-grained analysis of the effects of repeated stimulus presentation on ERPs within the parietal cluster identified in the mass univariate analysis (Fig. 5). First, we calculated ERPs separately for each presentation order (first versus second) and display format (real versus image) (Fig. 6A). Close inspection of Fig. 6 reveals that late ERPs over parietal cortex were stronger for objects on the second, versus initial, presentation (Fig. 6A, solid versus dashed lines), but this effect was most apparent for objects that were viewed *first* as a real object (Fig. 6A, solid blue versus solid red line). A 2 × 2 repeated measure analysis of variance revealed a significant interaction between display format and sequence of presentation [$F(1,23) = 19.549$, $p < .001$; Fig. 6C]. To decompose this interaction we computed the corresponding difference waveform (second minus first presentation) separately for (i) object images seen initially as real objects (Fig. 6B, pink line), and (ii) real objects seen initially as 2D images (Fig. 6B, cyan line). The resulting difference waveforms were significantly greater than zero for images seen initially as real objects [$t(23) = 5.479$, $p < .001$], but not for real objects seen initially as images [$t(23) = 0.450$, $p = .657$]. Taken together, therefore, the display format difference evident in the mass univariate ERP analysis are consistent with stronger object recollection after prior exposure to real objects versus images. This result is intriguing because it may reflect a neural signature of the mnemonic advantage for real objects versus images found in previous behavioral studies (Snow et al., 2014).

### 3.4. ERSP and ERP signatures of real-world objects are not explained by early ERPs

Finally, we ran a control analysis to determine the extent to which the unique neural signatures observed for real objects (versus images) in the central-ERSP and parietal-ERP analyses were independent of early signal differences related to stereopsis. To do this we re-examined the ERSP and ERP data after having removed trials that contributed to the relatively larger negativity in early occipital ERPs for real objects (Pegna et al., 2017). For each participant, we selected from the occipital ERP cluster (see Fig. 5, lower left panel) trials that fell within the upper, and lower, 45% of the amplitude distribution, for the 'real object' and 'image' conditions, respectively (Fig. 7A). Averaging the resulting trials in each condition confirmed that there were no differences in early visual ERPs [$t(23) = -0.109$, $p = .914$]. As such, the reduced data sets in each display format were indistinguishable based on early visual signatures commonly associated with stereopsis (Fig. 7A). Critically, to the extent that effects of display-format in the central-ERSP and parietal-ERP analyses reflect differences in early visual ERPs, they should not be apparent in the control analyses. On the contrary, in the central-ERSP analysis, several time-frequency clusters of significantly larger ERD for real objects versus images were identified within the μ frequency band, and in the β frequency band, replicating the original results (cluster-based permutation test: $n = 10000$, intensity threshold for cluster formation $\alpha = 0.001$, cluster size threshold $\alpha = 0.05$; Fig. 7B and Supplementary Table 4). Similarly, no ERS was observed at any time point or frequency within the analyzed time-window, underscoring again the directional specificity of the observed time-frequency perturbations. In the analysis of late parietal ERPs, amplitudes were marginally larger overall for images relative to real objects, even in the reduced dataset [$t(23) = 2.005$, $p = .028$, one-tailed], and again there was a significant interaction between display format and sequence of presentation [$F(1,23) = 4.678$, $p = .041$; Fig. 7C]. This pattern of results indicates that differences between real objects and images in early visual ERPs did not modulate later display-format related cortical brain dynamics.

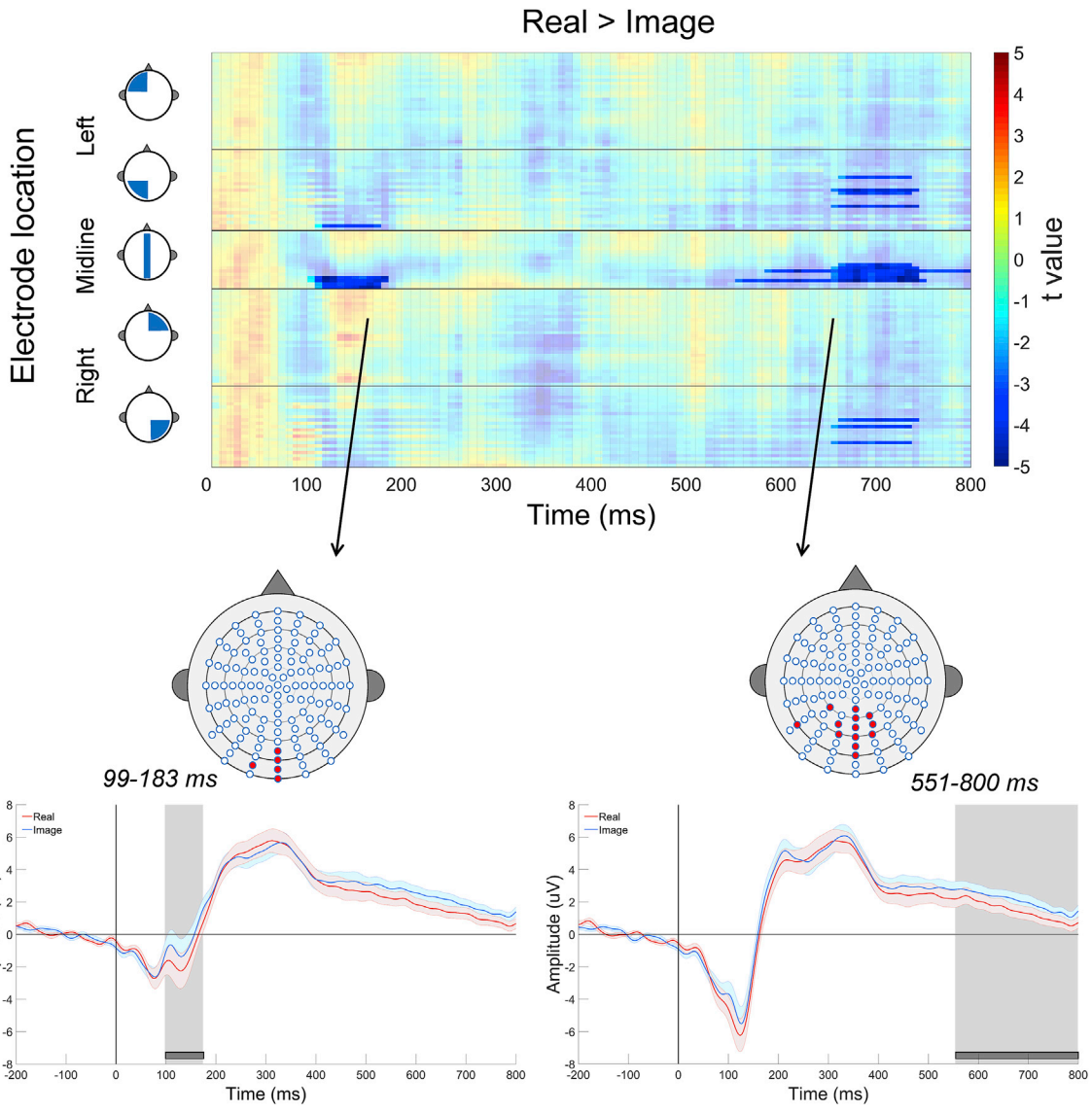


**Fig. 5.** Mass univariate analysis of event-related potentials (ERPs).
Mass univariate contrasts between display formats (real minus image) conducted at different electrodes (y-axis) and time-bins (x-axis). Color scale denotes t-values; saturated colors indicate statistically significant time-electrode clusters (corrected with cluster-based permutation tests). More positive ERPs for images versus real objects were observed early after stimulus onset in a cluster of electrodes over occipital cortex, and later in the post-stimulus period in a cluster of electrodes over parietal cortex (electrodes highlighted in red in the scalp maps). ERP traces in the lower panels represent averages across electrodes from the occipital (left) and parietal (right) clusters, respectively. Time labels and shaded areas indicate the time-period in which significant effects were observed within each cluster.

## 4. Discussion

A fundamental assumption in psychology and cognitive neuroscience has been that images of objects, which do not afford action, are processed similarly by the brain as are real-world solid objects. However, there is accumulating behavioral evidence that humans process real-world objects differently to stimuli presented in other display formats, including both 2-D planar (Chainay and Humphreys, 2001; Gerhard et al., 2016; Gomez et al., 2017; Humphrey et al., 1994; Romero et al., 2018; Snow et al., 2011, 2014) and 3-D stereoscopic images of objects (Gomez et al., 2017).The underlying neural mechanisms for these format-related effects on behavior have received scant investigation. Although real-world objects have been hypothesized to trigger stronger or more prolonged activation in visuo-motor networks involved in automatic action planning (Cisek and Kalaska, 2010; Gallivan et al., 2009, 2011b; Gomez et al., 2017), few studies have tested these ideas directly, most likely because of the difficulty of presenting real-world objects under controlled viewing conditions, and because of limitations in the temporal sensitivity of brain activity as measured by fMRI (Freud et al., 2017; Snow et al., 2011). Here, we leveraged the high temporal resolution of EEG to compare cortical brain responses to real-world objects versus matched high-resolution 2-D images of the same items.

Behaviorally, perceived effort-to-use was greater for real objects than images, particularly for high- (versus low-) effort objects, even though participants were not required to interact physically with any of the stimuli. On the one hand, these behavioral results may seem counterintuitive because if real objects automatically trigger motor preparation to act more so than images do, then effort-to-use judgements might be facilitated, thereby eliciting *lower* effort-to-use ratings. However, close inspection of Fig. 1C (left panel) shows that effort ratings for the different tools followed a sensible sequence from items that would be expected to be easy-versus items that are more effortful-to-use. Therefore, our finding that real objects elicited greater effort-to-use ratings than images do is consistent with the notion that real objects convey more precise or

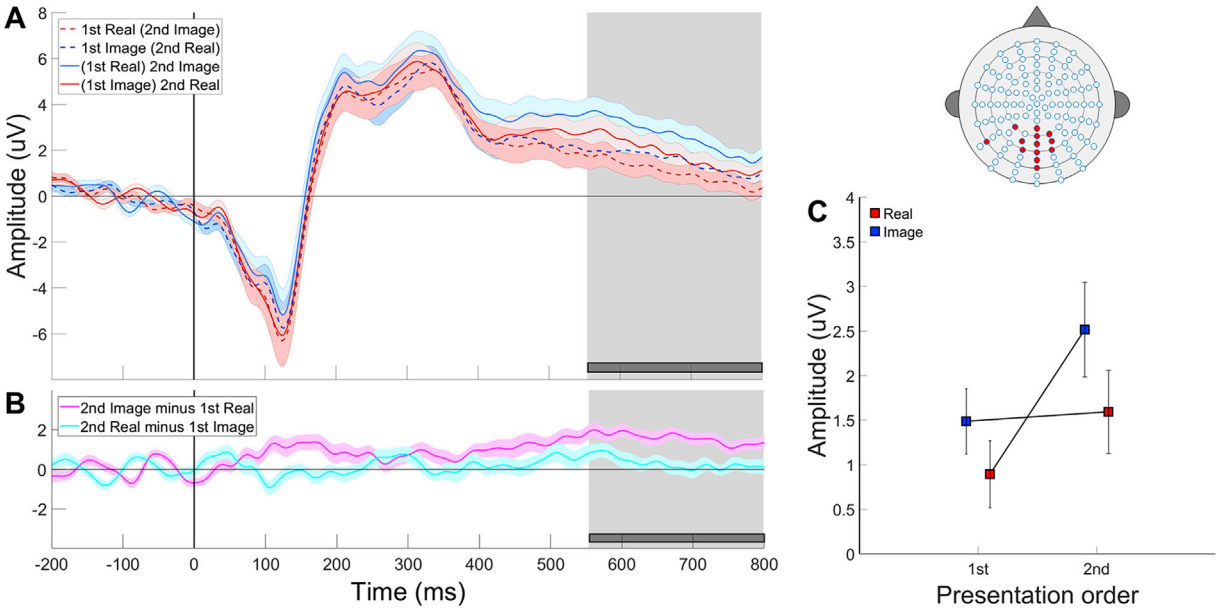


**Fig. 6.** Presentation-sequence analysis of parietal event-related potentials (ERPs).
*Panel A*. ERPs traces shown separately for stimuli in each display format and presentation order (first: dashed lines; second: solid lines). ERPs are drawn from the late parietal cluster identified in the mass univariate analysis in Fig. 5 (red electrodes in top right map). Shaded gray region denotes the time-range of significant effects.
*Panel B*. Difference ERP waveforms between the second versus first presentation of each object, displayed separately for the two combinations of display formats.
*Panel C*. Average ERP amplitude within the late parietal cluster of electrodes, displayed separately for stimuli in each display format and presentation order (error bars represent between-subject SEM).

detailed information about the actual physical requirements for interaction than do abstractions, thereby increasing (rather than reducing) anticipated exertion.

At the neural level, we were interested in whether real objects would elicit EEG responses that were similar or different to 2-D images of the same items. Overall EEG responses to the real objects and 2-D images were globally comparable; many of the characteristics of ERSPs were preserved across both stimulus formats. The fact that EEG measures were globally similar also underscores the fact that we controlled carefully our stimuli and design to ensure close matching between image and real objects. In the time-frequency domain, both real objects and images of objects elicited μ-band desynchronization in electrodes over centro-parietal cortex. Although desynchronization was observed within the μ band, and to a limited extent in the β frequency band (Turella et al., 2016; Zaepffel et al., 2013), there was no synchronization or desynchronization in the lower γ-band frequencies (30–50Hz), thus evincing a specific neural signature consistent with activation in visuo-motor networks involved in automatic action planning (Pineda, 2005).

Importantly, however, despite the global similarity of brain responses between real objects and images, there were key differences in cortical dynamics across the two display formats. First, in line with our predictions, real objects triggered more robust μ and β band desynchronization compared to the image displays. Second, we observed a significant difference in the strength of μ desynchronization between real objects and images over the putative left, but not the right, primary motor cortex. The lateralized focus of the μ desynchronization effects suggests that real objects elicit effector-specific differences in neural signals related to automatic action planning. The hemispheric specificity of the effect also argues against explanations based on lower-level visual differences between the stimuli, which should presumably yield a bilateral pattern. Interestingly, differences in ERD were observed after stimulus onset, but also after stimulus offset. It is possible that the early versus late temporal differences in ERD reflect the contribution of different cortical mechanisms involved in processing real objects and images.

Real objects also elicited ERPs that differed from those of images, although unlike the ERSPs, these differences were not lateralized. Specifically, the amplitude of late parietal ERPs was modulated by stimulus presentation order. In the well-known ERP signature of recollection known as the 'old/new effect' or 'late positive complex' or 'P600' (Donaldson and Rugg, 1999; Friedman and Johnson, 2000; Harris and Wilcox, 2009; Rugg and Curran, 2007; Rugg et al., 1998; Schendan and Kutas, 2003; Voss and Paller, 2008), late parietal ERPs for 'old' (i.e., previously seen) stimuli are more positive than those for 'new' (i.e., not previously seen) stimuli. In our study, late parietal ERPs were more positive when stimuli were viewed first as real-objects and then as images (compared to vice versa). This pattern in late ERPs suggests that objects were more memorable when they had been encountered initially as real-world objects and may reflect a striking neural correlate of the mnemonic advantage for real-world objects versus photographs and line drawings (Snow et al., 2014). Future research is required to determine whether there is a difference in behavioral measures of memory that correspond with those of the neural measures. It is interesting to speculate as to whether familiarity with an object (such as how to interact with a tool) could influence mnemonic effects such as those reported here. Future studies could examine whether brain response, or behavioral recall performance, are better for familiar versus novel or unfamiliar objects for which there may not be an internal model of how to interact with them.

Unlike studies of image vision in which stimulus presentation is entirely computer-controlled, working with real object displays presents a number of practical challenges, ranging from standardizing stimulus appearance and position, to controlling the order, onset and duration of the stimuli. Our control of the stimuli, procedure, and experimental design, preclude alternative explanations based on visual differences between the stimuli with respect to size, distance, viewpoint, color, or illumination. Moreover, both the onset and duration of stimulus presentation time was matched between display formats with millisecond precision on all trials. Importantly, we considered the possibility that the differences in cortical brain dynamics described above might reflect processing differences attributable to depth perception. Due to the lateral displacement of the left and right eyes, each retina receives visual information from a slightly different horizontal vantage point. The

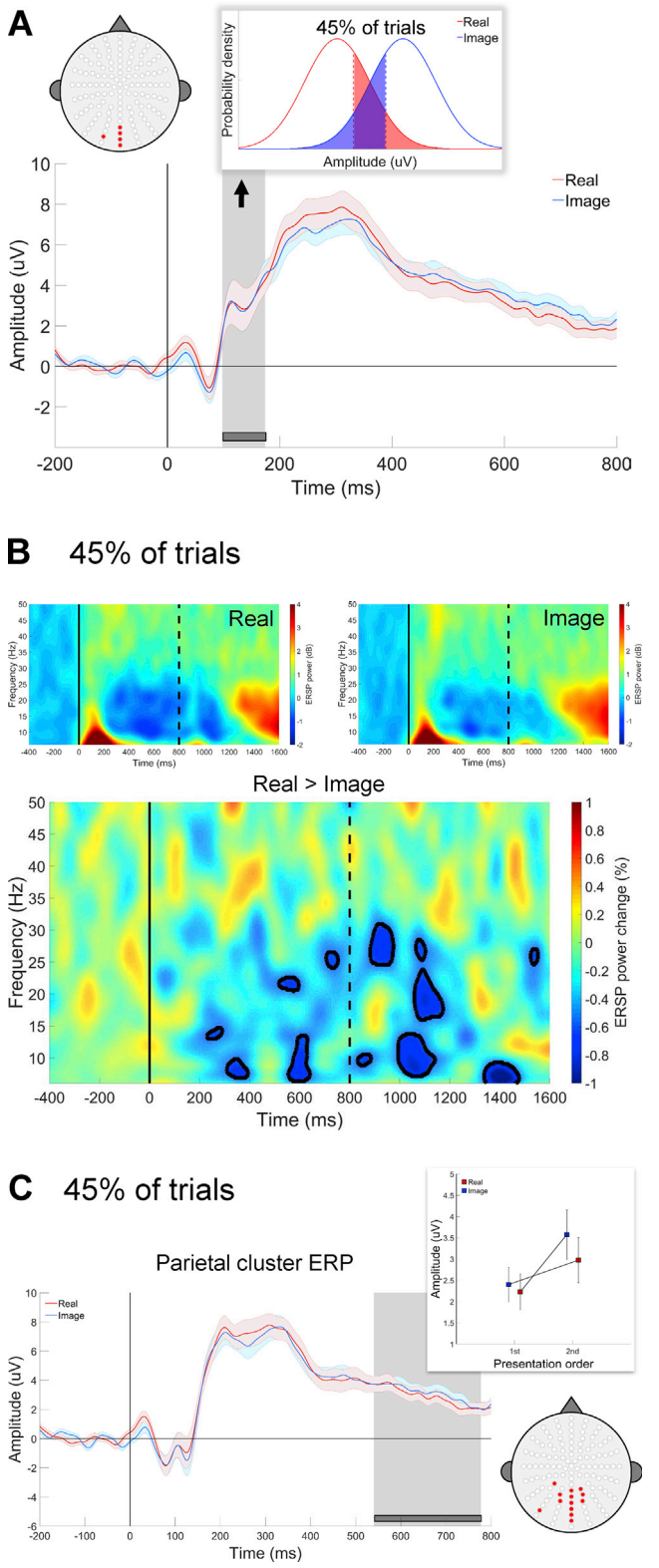


*(caption on next column)*

discrepancy between these different retinal images, known as binocular disparity, is resolved by the brain to produce a unitary sense of depth. However, binocular disparity (and therefore depth) is not conveyed by 2-D images because the *same* information is projected to each retina (Julez, 2006). In line with the inherent format-related differences in stereoscopic depth cues, we found that real objects (versus images) elicited a transient negativity of ERPs over occipital electrodes starting ~100 ms post-stimulus onset. This difference in early ERPs corresponds with previous reports of enhanced early negativity for images presented with, versus without, binocular disparity (Akay and Celebi, 2009; Gao et al., 2015; Kasai and Morotomi, 2001; Kasai et al., 2003; Pegna et al., 2017). Importantly, the format-dependent differences that we observed in ERSPs and late ERPs are unlikely to be related to the early ERP differences, because the effects were replicated when we analyzed *only* trials in which early ERPs were indistinguishable across display formats.

The results of the current study raise the question of whether real objects should be always used in research studies in place of images of objects. Although we found differences in cortical brain dynamics between real objects and images, there were also global similarities. For some areas of research, the differences described here may be critical for the interpretation of results and, if so, the use of real objects would provide an undoubted advantage over using images. However, for other areas of research the convenience of using images of objects balances the sacrifice in terms of measuring the exact activation pattern observed during normal use of an object. Here, we have highlighted the similarities and differences in brain responses to real-world objects and images so that researchers can make informed decisions when designing future studies. Our EEG results may have important implications for fMRI studies of image vision. Although the comparably slower time-scale of fMRI precludes a detailed analysis of temporal differences in cortical brain dynamics, 10Hz-desynchronization in the EEG signal is positively correlated with the magnitude of the fMRI BOLD signal (Lauf et al., 2003). As such, fMRI signals may be amplified for real objects compared to images, particularly when (as in most fMRI studies) the images are projected onto a mirror attached to the top of the head coil, so that distance, size and egocentric location of the stimulus are unknown. On the contrary, however, a previous slow event-related fMRI study by Snow et al. (2011) did not report differences in overall activation between real objects versus 2-D photographs of the same items. However, there are important differences between the fMRI study by Snow et al. (2011) and the current experiment. Participants in Snow et al.'s. (2011) study viewed the stimuli passively and the objects consisted of a variety of tool and non-tool objects; in the current study participants made action-related judgments about objects (tools) that have strong action associations.

**Fig. 7.** Control analysis.
*Panel A.* ERP waveforms from the occipital electrode cluster identified in the mass univariate analysis, but including a subset of 45% of the total trials for each subject corresponding to the right tail of the amplitude distribution for the real objects and the left tail for the images. When averaged together, trials in this subset show no difference within the occipital cluster time-window. This subset of trials was used to replicate the main ERSP and ERP analyses in order to test whether the original results held after parsing-out early ERP differences between display formats.
*Panel B.* Time-frequency ERSP power computed on the subset of 45% of trials identified as shown in Panel A. The stronger ERDs for real objects relative to images in the μ and β frequency bands illustrated in Fig. 2 was replicated here. The data for this analysis were noisier (consisting of only 45% of the total) and therefore the significant regions (highlighted by the black outlines; Supplementary Table 4) appear more scattered than those in Fig. 2, although very similar overall.
*Panel C.* ERPs from the parietal electrode cluster computed on the subset of 45% of trials identified as shown in Panel A. The ERP amplitude observed in the late time-window tended to be larger for images (marginally significant), and the significant interaction between presentation order and display format was replicated. This pattern confirms the results shown in Fig. 6.

The nature of the stimuli, as well as the task that participants perform, may have important effects on measured responses (e.g., see Freud et al., 2017).

In summary, these data provide critical empirical support for recent speculations that real-world objects elicit stronger and more prolonged neural responses in action-related visuo-motor networks than images do (Cisek and Kalaska, 2010; Gallivan et al., 2009; Gomez et al., 2017). The results provide new insights into the underlying neural mechanisms that drive the unique effects of real objects on human cognition, including eye movements in infants (Gerhard et al., 2016), object recognition (Chainay and Humphreys, 2001; Humphrey et al., 1994), attention (Gomez et al., 2017), memory (Snow et al., 2014), and decision-making (Mischel and Moore, 1973; Romero et al., 2018). Compared to images, real objects may trigger more vivid motor imagery, more detailed or well-specified action plans, and/or a greater number of competing action plans that must be resolved prior to decision (Gallivan et al., 2009, 2011a; Gomez et al., 2017). Recent behavioral evidence has shown that real objects influence behavior differently to 2-D versus 3-D stereoscopic images of the objects, and that these effects are eliminated when the real objects are presented out of reach or behind a transparent barrier that prevents potential in-the-moment interaction with the objects (Gomez et al., 2017). To the extent that the neurophysiological modulations described here reflect the same underlying mechanisms, the enhanced visuo-motor responses for real objects (versus images) are likely to reflect the genuine and automatic affordances that real objects offer the observer for manual interaction (Gibson, 1979). Whether these neural signatures of realness reflect quantitative or qualitative differences in neural action codes, and whether similar signatures of realness are apparent in the context of virtual- (Cardellicchio et al., 2011; Wamain et al., 2016) or augmented-reality stimuli, particularly those that afford manual interaction with the objects, remain intriguing questions for future research. Given findings from recent behavioral studies (Gomez et al., 2017), a critical next step is to determine whether the mechanisms that drive amplified μ desynchronization for real objects (versus 2-D images) reflect reachability, tangibility, or both.

## Acknowledgements

This work was supported by grants from the National Science Foundation (grant number 1632849 to J.C.S.); the National Eye Institute of the National Institutes of Health (grant number R01EY026701 to J.C.S.); and the National Institute of General Medical Sciences of the National Institutes of Health (grant number P20 GM103650). The content is solely the responsibility of the authors and does not necessarily represent the official views of the NSF or NIH. We would like to thank Shane Jacobs for assistance with data collection, Luca Pion-Tonachini for coding advice, and Marlene Behrmann, Michael Crognale, Sara Fabbri and Scott Makeig for helpful discussion.

## Appendix A. Supplementary data

Supplementary data to this article can be found online at https://doi.org/10.1016/j.neuroimage.2019.02.026.

## References

Akay, A., Celebi, G., 2009. A brain electrophysiological correlate of depth perception. Neuroscience 14, 139–142.
Basar, E., Basar-Eroglu, C., Karakas, S., Schurmann, M., 1999. Are cognitive processes manifested in event-related gamma, alpha, theta and delta oscillations in the EEG? Neurosci. Lett. 259, 165–168.
Behmer Jr., L.P., Jantzen, K.J., 2011. Reading sheet music facilitates sensorimotor mu-desynchronization in musicians. Clin. Neurophysiol. 122, 1342–1347.
Blair, R.C., Karniski, W., 1993. An alternative method for significance testing of waveform difference potentials. Psychophysiology 30, 518–524.
Brady, T.F., Konkle, T., Alvarez, G.A., Oliva, A., 2008. Visual long-term memory has a massive storage capacity for object details. Proc. Natl. Acad. Sci. U. S. A. 105, 14325–14329.
Brady, T.F., Stormer, V.S., Alvarez, G.A., 2016. Working memory is not fixed-capacity: more active storage capacity for real-world objects than for simple stimuli. Proc. Natl. Acad. Sci. U. S. A. 113, 7459–7464.
Cardellicchio, P., Sinigaglia, C., Costantini, M., 2011. The space of affordances: a TMS study. Neuropsychologia 49, 1369–1372.
Chainay, H., Humphreys, G.W., 2001. The real-object advantage in agnosia: evidence for a role of surface and depth information in object recognition. Cogn. Neuropsychol. 18, 175–191.
Cisek, P., Kalaska, J.F., 2010. Neural mechanisms for interacting with a world full of action choices. Annu. Rev. Neurosci. 33, 269–298.
Delorme, A., Makeig, S., 2004. EEGLAB: an open source toolbox for analysis of single-trial EEG dynamics including independent component analysis. J. Neurosci. Methods 134, 9–21.
Donaldson, D.I., Rugg, M.D., 1999. Event-related potential studies of associative recognition and recall: electrophysiological evidence for context dependent retrieval processes. Brain Res Cogn Brain Res 8, 1–16.
Freud, E., Macdonald, S.N., Chen, J., Quinlan, D.J., Goodale, M.A., Culham, J.C., 2017. Getting a grip on reality: grasping movements directed to real objects and images rely on dissociable neural representations. Cortex 98, 34–48.
Friedman, D., Johnson Jr., R., 2000. Event-related potential (ERP) studies of memory encoding and retrieval: a selective review. Microsc. Res. Tech. 51, 6–28.
Gallivan, J.P., Cavina-Pratesi, C., Culham, J.C., 2009. Is that within reach? fMRI reveals that the human superior parieto-occipital cortex encodes objects reachable by the hand. J. Neurosci. 29, 4381–4391.
Gallivan, J.P., McLean, A., Culham, J.C., 2011a. Neuroimaging reveals enhanced activation in a reach-selective brain area for objects located within participants' typical hand workspaces. Neuropsychologia 49, 3710–3721.
Gallivan, J.P., McLean, D.A., Valyear, K.F., Pettypiece, C.E., Culham, J.C., 2011b. Decoding action intentions from preparatory brain activity in human parieto-frontal networks. J. Neurosci. 31, 9599–9610.
Gao, F., Cao, B., Cao, Y., Li, F., Li, H., 2015. Electrophysiological evidence of separate pathways for the perception of depth and 3D objects. Int. J. Psychophysiol. 96, 65–73.
Gerhard, T.M., Culham, J.C., Schwarzer, G., 2016. Distinct visual processing of real objects and pictures of those objects in 7- to 9-month-old infants. Front. Psychol. 7, 827.
Gibson, J.J., 1979. The Ecological Approach to Visual Perception. Houghton Mifflin, Boston, MA.
Gomez, M.A., Skiba, R.M., Snow, J.C., 2017. Graspable objects grab attention more than images do. Psychol. Sci. 956797617730599.
Grandchamp, R., Delorme, A., 2011. Single trial normalization for event-related spectral decomposition reduces sensitivity to noisy trials. Front. Psychol. 2, 236.
Groppe, D.M., Urbach, T.P., Kutas, M., 2011. Mass univariate analysis of event-related brain potentials/fields I: a critical tutorial review. Psychophysiology 48, 1711–1725.
Guthrie, D., Buchwald, J.S., 1991. Significance testing of difference potentials. Psychophysiology 28, 240–244.
Handy, T.C., Grafton, S.T., Shroff, N.M., Ketay, S., Gazzaniga, M.S., 2003. Graspable objects grab attention when the potential for action is recognized. Nat. Neurosci. 6, 421–427.
Hari, R., 2006. Action-perception connection and the cortical mu rhythm. Prog. Brain Res. 159, 253–260.
Harris, J.M., Wilcox, L.M., 2009. The role of monocularly visible regions in depth and surface perception. Vis. Res. 49, 2666–2685.
Homan, R.W., Herman, J., Purdy, P., 1987. Cerebral location of international 10-20 system electrode placement. Electroencephalogr. Clin. Neurophysiol. 66, 376–382.
Humphrey, G.K., Goodale, M.A., Jakobson, L.S., Servos, P., 1994. The role of surface information in object recognition: studies of a visual form agnosic and normal subjects. Perception 23, 1457–1481.
Julez, B., 2006. Foundations of Cyclopean Perception, 1 ed. The MIT Press.
Kasai, T., Morotomi, T., 2001. Event-related brain potentials during selective attention to depth and form in global stereopsis. Vis. Res. 41, 1379–1388.
Kasai, T., Morotomi, T., Katayama, J., Kumada, T., 2003. Attending to a location in three-dimensional space modulates early ERPs. Brain Res Cogn Brain Res 17, 273–285.
Khaligh-Razavi, S., Cichy, R.M., Pantazis, D., Oliva, A., 2018. Tracking the spatiotemporal neural dynamics of real-world object size and animacy in the human brain. J. Cognit. Neurosci. 30, 1559–1576.
Kleiner, M., Brainard, D., Pelli, D., Ingling, A., Murray, R., Broussard, C., 2007. What's new in Psychtoolbox-3. Perception 36, 1.
Klimesch, W., 1999. EEG alpha and theta oscillations reflect cognitive and memory performance: a review and analysis. Brain Res Brain Res Rev 29, 169–195.
Konkle, T., Brady, T.F., Alvarez, G.A., Oliva, A., 2010. Conceptual distinctiveness supports detailed visual long-term memory for real-world objects. J. Exp. Psychol. Gen. 139, 558–578.
Konkle, T., Oliva, A., 2011. Canonical visual size for real-world objects. J. Exp. Psychol. Hum. Percept. Perform. 37, 23–37.
Konkle, T., Oliva, A., 2012. A real-world size organization of object responses in occipitotemporal cortex. Neuron 74, 1114–1124.
Laufs, H., Kleinschmidt, A., Beyerle, A., Eger, E., Salek-Haddadi, A., Preibisch, C., Krakow, K., 2003. EEG-correlated fMRI of human alpha activity. Neuroimage 19, 1463–1476.
Lee, S.H., Kravitz, D.J., Baker, C.I., 2012. Disentangling visual imagery and perception of real-world objects. Neuroimage 59, 4064–4073.
Logothetis, N.K., Pauls, J., Augath, M., Trinath, T., Oeltermann, A., 2001. Neurophysiological investigation of the basis of the fMRI signal. Nature 412, 150–157.

Makeig, S., 1993. Auditory event-related dynamics of the EEG spectrum and effects of exposure to tones. Electroencephalogr. Clin. Neurophysiol. 86, 283–293.
Makeig, S., Bell, A.J., Jung, T.-P., Sejnowski, T.J., 1996. Independent component analysis of electroencephalographic data. Adv. Neural Inf. Process. Syst. 8, 145–151.
Makeig, S., Westerfield, M., Jung, T.P., Enghoff, S., Townsend, J., Courchesne, E., Sejnowski, T.J., 2002. Dynamic brain sources of visual evoked responses. Science 295, 690–694.
Marini, F., Breeding, K.A., Snow, J.C., 2019. Dataset of 24-subject EEG recordings during viewing of real-world objects and planar images of the same items. Data in Brief, 103857.
Maris, E., Oostenveld, R., 2007. Nonparametric statistical testing of EEG- and MEG-data. J. Neurosci. Methods 164, 177–190.
McNair, N.A., Behrens, A.D., Harris, I.M., 2017. Automatic recruitment of the motor system by undetected graspable objects: a motor-evoked potential study. J. Cognit. Neurosci. 29, 1918–1931.
Mischel, W., Moore, B., 1973. Effects of attention to symbolically presented rewards on self-control. J. Pers. Soc. Psychol. 28, 172–179.
Muthukumaraswamy, S.D., Johnson, B.W., 2004. Primary motor cortex activation during action observation revealed by wavelet analysis of the EEG. Clin. Neurophysiol. 115, 1760–1766.
Muthukumaraswamy, S.D., Johnson, B.W., McNair, N.A., 2004. Mu rhythm modulation during observation of an object-directed grasp. Brain Res Cogn Brain Res 19, 195–201.
Nako, R., Smith, T.J., Eimer, M., 2015. Activation of new attentional templates for real-world objects in visual search. J. Cognit. Neurosci. 27, 902–912.
Neuper, C., Pfurtscheller, G., 2001. Event-related dynamics of cortical rhythms: frequency-specific features and functional correlates. Int. J. Psychophysiol. 43, 41–58.
Nyström, P., Ljunghammar, T., Rosander, K., von Hofsten, C., 2011. Using mu rhythm desynchronization to measure mirror neuron activity in infants. Dev. Sci. 14, 327–335.
Pegna, A.J., Darque, A., Roberts, M.V., Leek, E.C., 2017. Effects of stereoscopic disparity on early ERP components during classification of three-dimensional objects. Q. J. Exp. Psychol. 1–35.
Perry, A., Stein, L., Bentin, S., 2011. Motor and attentional mechanisms involved in social interaction – evidence from mu and alpha EEG suppression. Neuroimage 58, 895–904.
Perry, A., Bentin, S., 2009. Mirror activity in the human brain while observing hand movements: a comparison between EEG desynchronization in the μ-range and previous fMRI results. Brain Res. 1282, 126–132.
Pfurtscheller, G., 2001. Functional brain imaging based on ERD/ERS. Vis. Res. 41, 1257–1260.
Pfurtscheller, G., Brunner, C., Schögl, A., Lopes da Silva, F.H., 2006. Mu rhythm (de) synchronization and EEG single trial classification of different motor imagery tasks. Neuroimage 31, 153–159.
Pfurtscheller, G., Neuper, C., Andrew, C., Edlinger, G., 1997. Foot and hand area mu rhythms. Int. J. Psychophysiol. 26, 121–135.
Pineda, J.A., 2005. The functional significance of mu rhythms: translating "seeing" and "hearing" into "doing. Brain Res Brain Res Rev 50, 57–68.
Pineda, J.A., Giromini, L., Porcelli, P., Parolin, L., Viglione, D.J., 2011. Mu suppression and human movement responses to the Rorschach test. Neuroreport 22, 223–226.
Proverbio, A.M., Adorni, R., D'Aniello, G.E., 2011. 250ms to code for action affordance during observation of manipulable objects. Neuropsychologia 49, 2711–2717.
Proverbio, A.M., 2012. Tool perception suppresses 10-12Hz μ rhythm of EEG over the somatosensory area. Biol. Psychol. 91, 1–7.
Romero, C.A., Compton, M.T., Yang, Y., Snow, J.C., 2018. The real deal: Willingness-to-pay and satiety expectations are greater for real foods versus their images. Cortex 107, 78–91.
Rugg, M.D., Curran, T., 2007. Event-related potentials and recognition memory. Trends Cognit. Sci. 11, 251–257.
Rugg, M.D., Mark, R.E., Walla, P., Schloerscheidt, A.M., Birch, C.S., Allan, K., 1998. Dissociation of the neural correlates of implicit and explicit memory. Nature 392, 595–598.
Schendan, H.E., Kutas, M., 2003. Time course of processes and representations supporting visual object identification and memory. J. Cognit. Neurosci. 15, 111–135.
Snow, J.C., Pettypiece, C.E., McAdam, T.D., McLean, A.D., Stroman, P.W., Goodale, M.A., Culham, J.C., 2011. Bringing the real world into the fMRI scanner: repetition effects for pictures versus real objects. Sci. Rep. 1, 130.
Snow, J.C., Skiba, R.M., Coleman, T.L., Berryhill, M.E., 2014. Real-world objects are more memorable than photographs of objects. Front. Hum. Neurosci. 8, 837.
Suzuki, M., Noguchi, Y., Kakigi, R., 2014. Temporal dynamics of neural activity underlying unconscious processing of manipulable objects. Cortex 50, 100–114.
Turella, L., Tucciarelli, R., Oosterhof, N.N., Weisz, N., Rumiati, R., Lingnau, A., 2016. Beta band modulations underlie action representations for movement planning. Neuroimage 136, 197–207.
Voss, J.L., Paller, K.A., 2008. Brain substrates of implicit and explicit memory: the importance of concurrently acquired neural signals of both memory types. Neuropsychologia 46, 3021–3029.
Wamain, Y., Gabrielli, F., Coello, Y., 2016. EEG mu rhythm in virtual reality reveals that motor coding of visual objects in peripersonal space is task dependent. Cortex 74, 20–30.
Wamain, Y., Sahaï, A., Decroix, J., Coello, Y., Kalénine, S., 2018. Conflict between gesture representations extinguishes μ rhythms desynchronization during manipulable object perception: an EEG study. Biol. Psychol. 132, 202–211.
Zaepffel, M., Trachel, R., Kilavik, B.E., Brochier, T., 2013. Modulations of EEG beta power during planning and execution of grasping movements. PLoS One 8, e60060.